Structural, Mechanical and Electrical Properties of Sputter Coated Copper Thin Films on Poly Ethylene Terephthalate

A. Atta (aamahmad@ju.edu.sa)
Physics Department, College of Science, Jouf University, P.O. Box:2014, Sakaka, Saudi Arabia.
E. Abdeltwab
Physics Department, College of Science, Jouf University, P.O. Box:2014, Sakaka, Saudi Arabia.
Alpan Bek
Physics Department, Middle East Technical University (METU), 06800 Ankara, Turkey

Research Article

Keywords: Deposition, CuNPs, PET, Structural, Mechanical, Electrical

Posted Date: February 13th, 2021

DOI: https://doi.org/10.21203/rs.3.rs-220271/v1

Abstract

Copper (Cu) thin films are deposited on polyethyleneterephthalate (PET) substrate using ion-beam-sputtering technique. The formation of Cu thin films is successful confirmed as investigated by X-ray diffraction (XRD). Surface morphology of Cu/PET is studied by atomic force microscopy (AFM). The AFM results show that Cu film dewets PET surface and the surface roughness increased from 22.6 nm for PET to 45.3 nm after 40min of deposited Cu/PET. The sheet resistance decreases from $5.16x10^{4}\Omega$ to $1.3x10^{4}\Omega$ and resistivity decreases from $2.3x10^{-2}\Omega.cm$ to $1.77x10^{-2}\Omega.cm$, as the Cu deposition time increases from 20min to 60min. The Young's modulus increases from 2.82GPa to 2.96GPa and the adhesion force enhanced from 14.7nN to 29.90nN after 40min of Cu deposition. The DC electrical conductivity at 300V is improved from $1.75x10^{-8}$ $S.cm^{-1}$ to $3.57x10^{-8}$ $S.cm^{-1}$ after 60min of Cu deposition. The results show that ion beam deposition of Cu on flexible PET platform clearly exhibits improvement over pristine PET in the mechanical and electrical properties which renders it useful for electronics applications.

1. Introduction

Fabrication of stable flexible conductive thin films is a relatively new area of research which promises improvement in the electrical and mechanical properties of candidate polymer substrates for applicable electronic devices [1–2]. The advantages for fabrication of conductive thin films on polymer substrates are combined the polymer flexibility with metal conductivity properties [3]. There are numerous different coating techniques capable of fabricating thin conducting films on polymer substrates. Ion beam assisted sputtering technique stands out for its capacity to generate large impact momentum and linear energy transfer of deposited species on the substrate, yielding superior mechanical stability of the fabricated film [4–5].

The interaction between beam irradiation and polymer surface during deposition process can be tuned for treating polymer surface to adjust their surface energy, surface conductivity and adhesion properties [6–8]. Bertrand et al. studied the interface formation between Cu with PET and PMMA films with low energy ion beam irradiation. They found that without surface activation, Cu atoms interact only very weakly with both polymer surfaces [9]. The deposition based metallic thin-films for electronic devices should have a low concentration of defects, good conductivity and high purity [10].

In recent years, researchers focus more on low dimensional conductors than bulk conductors, since low dimensionality of materials present them novel properties [11] such as superior yield strength [12] and in case of nanotubes even lower electrical resistance [13]. Intriguing properties of deposited metallic thin-films have led to different applications such as memory devices [14], micro-electro-mechanical systems (MEMS) [15], and optical devices [16]. Huang et al. fabricated Cu doped ultra-thin Ag transparent conductive films on glass and PET substrates. They recorded Cu:Ag thin films revealed excellent thermal, chemical and mechanical stability; and the flexible polymer solar cells using Cu:Ag electrodes have

reached a conversion efficiency of 7.53% [17]. Exemplary metals applied as conductivity promoters in electronic devices are silver, gold, copper and aluminum [18–19].

Recently, Cu thin films, chiefly on flexible polymer substrates such as PET, have become of high importance for flexible printed circuit boards [20]. The fabrication of metal thin-films on polymer substrates is studied in many different configurations such as copper on PTFE [21], copper on polyimide [22], silver/fluorocarbon nanocomposites on PET [23], aluminum on PET [24] and silver on PET [25], etc. Numerous parameters can affect the film structure, such as deposition time, gas type, gas pressure, substrate type, and the film thickness [26–28].

This study focuses physical ion beam sputtering method for deposition of Cu on PET. An advantage of physical deposition is facile control of Cu/PET properties by adjustment of deposition conditions. The structural, morphological and electrical properties of Cu deposited PET will be discussed. The aim of the present work is to point modification directions of the PET properties by ion beam deposition of Cu to meet requirements for its wide use in high technology applications.

2. Materials And Methods

2.1 Ion source sputtering system

The deposition processes were carried out using a home-designed ion beam sputtering instrument, which is described elsewhere [29]. A positive potential is applied by a DC power supply for initiating the discharge process between an anode and a cathode which is linked to the earth as shown in Fig. 1. A negative potential is applied to the extraction electrode by another DC power supply to extract the ion beam. Cu films are deposited on PET substrates at sputtering durations of 20, 40 and 60 minutes. The copper targets were placed by 45º angle with the beam trajectory of the ion source in the sputtering system. The sputtering process was carried out at 3 keV beam energy, 200 μA/cm^2 current density and 2x10^{-4} mbar argon base gas pressure.

2.2 Characterization techniques

PET substrate with 40 μm thickness and 1.5 cm x 1.5 cm dimension is ultrasonically cleaned in ethyl and methyl alcohol to remove organics, dried at 50 ºC in an oven for 30 min, and dried in air. These substrates are supplied from National Centre for Radiation Research and Technology (NCRRT), Cairo, Egypt.

The structure of Cu on PET is characterized using a fully computerized X-ray diffractometer, Shimadzu XRD-6000 in 2θ range from 4º – 90º at a scan rate of 2°/min. The changes in surface morphology and roughness of Cu on PET surface are investigated with AFM (JPK Nanowizard II, Berlin, Germany). The average value of surface roughness is estimated by scanning at 3 different places on the sample. The mechanical parameters, the adhesion force and Young's modulus, of Cu on PET were measured by AFM in non-contact mode by measuring the force-distance curves. The resistivity and sheet resistance of

Cu/PET are measured using the four-point probe (4PP) geometry. The DC electrical conductivity for PET and metalized Cu/PET are carried out in a cell with brass electrodes using A Keithley-617 electrometer at room temperature for measuring current-voltage characteristic curve. The transmittance spectra of pristine PET and Cu/PET are recorded using an UV–VIS spectrophotometer (JASCO V-670) in the wavelength range of 200 nm to 900 nm.

3. Results And Discussion

3.1 Structural investigation of Cu/PET film.

Fig.2 indicates XRD pattern of pristine PET and 60 min of Cu/PET films. For pristine PET is one strong peak at 2θ~25.70^{o}, while for Cu/PET pattern is one intensive peak for PET at 2θ~25.78 ^{o} and furthermore three peaks of Cu are (111), (200) and (220) planes at 2q ~ 43.32º, 50.38 and 74.04 respectively, which indicate successful formation of Cu nanoparticles (CuNPs) on PET. From XRD, the crystallite size D of the deposited Cu is estimated by using Debye-Scherer formula $D = 0.9\frac{\lambda}{\beta}cos\,\theta$ where b is full width at half maximum, l is wavelength of X-rays and q is diffraction angle. The average Cu thin film crystallite size is found to be 35.7 nm. As a confirmation, we would like to note that Liu et al. [30] estimated the average size of Cu (111) as 31.06 nm using Scherer equation. They identified that the deposited Cu on PET exhibited a characteristic face-centered cubic crystalline structure, which could imply the perfect conductive property of copper-plated polyester fabrics.

It is observed that the deposited Cu does not change the PET preferred orientation, but changed the PET peak intensity as shown in Fig.2. The enhancement of the PET peak intensity with deposited Cu implies a possible improvement of Cu/PET composite film crystallinity in comparison with the pure PET. Elsewhere, such behavior is found due to the Cu effect, which increases the effective delocalization and ordering of PET polymer chain [31]. For comparative results, Atta succeed for deposited copper nanoparticles (CuNPs) on PET substrate using cold cathode ion source sputtering technique, he estimated the crystallite size of the deposited Cu is in range of 31 nm [21]. Similarly, Oh et al. successfully fabricated Ag/PET, and they recorded that the effect of particle size and film thickness leads to variations in the polymer properties [32].

3.2 UV-Vis transmission of Cu/PET film.

Fig. 3 shows the UV/Vis transmission of pristine PET and 60 min Cu/PET films as a function of the wavelength (λ). It is clear from Fig.3 that in case of pristine PET, the transmission intensity is approximately 78% at λ=900 nm, with a little reduction at low wavelengths, which supported that PET is almost of transparent nature. For Cu/PET, the transmission decreases and hits 2.3% at the same wavelength λ= 900 nm. This reduction in transmittance after deposition is due to nucleation and coalescence of copper nuclei which results in morphological modification. This indicates a good miscibility between Cu and PET chains and supports XRD pattern and AFM images. It is concluded that

the amount of optical transmission depends on the defect state and the reduction in the disorder structure [33] due to the deposited CuNPs. The CuNPs exhibited transmittance band around 580 nm, related to conduction electrons excitation of the Cu metal NPs after their unique interaction with the electromagnetic light field. The recorded UV/Vis transmission results indicate that Cu/PET composite films offer good performance in terms of UV light shielding combined with reasonable transparency in the visible region, as well as flexibility of the films [34].

3.3 Surface morphology properties of Cu/PET films.

Fig.4 presents AFM images of pristine PET and Cu/PET films. The surface morphology of pristine PET is almost smooth with tiny grains as in Fig. 4a, while after 20 min deposition, dewetting of Cu thin-film begins with an increase in the surface roughness and partially linked nanostructures are formed [35]. The Cu thin-film on the surface becomes discontinuous and the structures made of percolated grains are formed as shown in Fig.4b and by increasing the deposition time to 40 min, small grains gradually combine producing bigger grains as observed in Fig. 4c. Finally, with increasing deposition time to 60 min, the grains become larger and start to create combined clusters as in Fig.4d. It is clearly observed that CuNPs are uniformly and continuously dispersed on PET surface. These AFM images confirm that the PET mechanical properties are improved with Cu deposition, as will be discussed in the adhesion force and Young's modulus section.

In order to obtain more detailed of surface structure analysis, we determined the relative grain size of CuNPs deposited PET substrate as shown in Fig.5, which obtained from AFM images. As observed from Fig.4, the Cu grains are covering the PET substrates with no cracks and smoothly distributed with uniform symmetrical shape. The recorded Cu grain size is decreased with influence copper deposition time as shown in Fig.5. It can be observed that in the initial phase of the deposition, after 20 min of copper deposition, there forms a relatively large scale grain, particularly of elliptical shape with major axis lengths about 400 nm. With more deposition time, reduces in size to around 100 nm after 40 min and to around 50 nm after 60 min, this value of 50 nm nearly at the same order as the pristine PET. It is observed the Cu size grain value nearly matches the calculated crystallite size of Cu coated PET, which calculated previously from XRD. It can concluded, as the deposition time increases, the grain shapes change from being highly elliptical to circular as demonstrated in AFM images Fig.4, and the grain size decreases from micro-meter scale to nano-scale as listed in Fig 5.

The root mean square surface roughness of the PET and Cu/PET films are shown in Fig. 6 and listed in Table1. When the deposition time increases from 20 to 40 min, with scan area of 3.0 μm x 3.0 μm, the roughness increases from 22.6 to 45.9 nm and then decreased to 34.5 nm by increasing the deposition time to 60 min as listed in Table 1. The variation of roughness shows that the coating is not a big influence on the substrate surface roughness. Xiong et al. fabricated transparent and conductive Cu/In:SnO using atomic layer deposition (ALD) method. They recorded that the deposited Cu film with a thickness of 10 nm showed excellent surface morphology with roughness value of 0.62 ± 0.03 nm [36].

3.4 Mechanical properties of Cu/PET films.

In view of a variety of scientific and technological applications of metal nanoparticles coated polymeric materials, we present here an experimental methodology based on the force mode of AFM to measure the mechanical properties of PET and Cu/PET films. The mechanical properties such as Young's modulus and adhesion force are investigated using AFM in contact mode for AFM tip interaction with PET surface [37]. The adhesion force and Young's modulus of Cu on PET are shown in Fig.6 and listed in Table 1. The adhesion force is increased from 14.72 nN for pristine PET to 29.92 nN at 40 min Cu/PET, and then decreases to 11.49 nN for 60 min Cu/PET. It's important to note that such a behavior of the nanostructures material prevails up to an optimized threshold value of Cu deposition time with the polymer matrix. Beyond that value of coating, there occurs a decrease in the degree of adhesion, and hence the composites would adopt a lesser elastic behavior. At a further increase of CuNPs concentration, the CuNPs tend to interact among themselves through their electronic cloud, this results in overall influence in elastic as well as mechanical properties behavior [38].

The changes in surface morphology as investigated by AFM, contributes in the Cu/PET adhesion force enhancement. In order to increase interlocking of Cu and PET binding forces, it is important to form polymer chain clusters in initial stage of film deposition with small circular island distribution. The Cu mobility is strongly influenced by the deposition time, which influences PET structure defects density and/or ion beam interaction effects. Therefore, the sputtering rate gets changed and more Cu atoms are subsequently dislodged at longer deposition times [39]. According to AFM results, the deposition of a Cu thin-film is a powerful tool for lending sufficient adhesion properties to PET substrates. The CuNPs, which is around 37 nm as recorded by XRD, are in compact arrangement that leads to high PET adhesion force.

The Young's modulus is increased from 2.82 GPa for pristine PET to 2.96 GPa for 40 min Cu/PET. This improvement is because of the layered structure as observed by AFM, which completely cover the PET substrate and improved the connectivity of the Cu-PET film [40]. Strong mechanical adhesion between the Cu and PET is produced due to increase in nanostructure surface area, and subsequent improvement of the adhesion force. These improvements in mechanical properties indicate that this simple home-made ion beam sputtering system is successful in fabrication of a flexible Cu/PET with good adhesion characteristics.

3.4 Electrical properties of Cu/PET films.

The sheet resistance and surface resistivity for Cu/PET with deposition times from 20 to 60 min are given in Table 1. The sheet resistance of Cu /PET decreases from $5.16x10^4$ Ω to $1.3x10^4$ Ω and the surface resistivity decreases from $2.34x10^{-2}$ Ω.cm to $1.77x10^{-2}$ Ω.cm, when the deposition time increases from 20 to 60 min. This reduction in shear resistance and surface resistivity is attributed to the fact that when the quantity of CuNPs increase on PET, the Cu film becomes more continuous. And at short deposition time, the sputtered Cu ions cannot gain sufficient energy to modify the bond direction among the Cu film atoms and PET substrate. This leads to some difficulty in making large nucleated grains to grow. Increasing the deposition time to 40 min leads to connection of islands and a layered film, which acts as a conducting path [41]. This improves the carrier mobility and subsequently decreases the sheet

resistance and film resistivity. However, at 60 min Cu/PET, unconnected Cu islands form due to high surface diffusion of CuNPs on the PET surface, which increases the resistivity of the Cu/PET film. So, the optimum duration for Cu to sufficiently have effective nucleation and improved connectivity on PET substrate is 40 min [42].

Chen et al. fabricated Cu-coated glass fabric using electroless plating method. These fabrics possessed excellent conductivity of the composites as shielding materials with resistivity down to 2.57×10^{-3} Ω.cm [43]. During deposition, initially there exists a low adherence between Cu films and PET substrate, which causes a low mobility and a low surface conductivity, due to active contribution of the grain boundaries in charge carrier scattering [44]. By increasing duration, more uniform film with less PET roughness is obtained, leading to increased surface conductivity [45].

Table 1: The adhesion force, Young's modulus, roughness, sheet resistance and surface resistivity of pristine PET and of Cu/PET films

	Young's modulus (GPa)	Adhesion force (nN)	Roughness (nm)	Sheet resistance (Ω)	Resistivity (Ω. cm)
Pristine PET	2.82±0.48	14.72±0.86	22.6±0.4	2.57E+11	4.61E+07
20 min Cu/PET	2.86±0.28	24.49±0.98	24.9±0.3	5.16E+04	2.34E-02
40 min Cu/PET	2.96±0.46	29.92±0.58	45.3±0.6	9.22E+02	8.36E-04
60 min Cu/PET	0.96±0.18	11.49±0.91	34.5±0.5	1.30E+04	1.77E-02

In order to investigate the effect of Cu deposition on PET conductivity, the current – voltage I-V characteristic measurements curve are performed. The current is measured in applied voltage range of 0–300 V as shown in Fig.7. It is observed that the current increases smoothly with increasing applied voltage, which confirms that the flow of current through metallized polymer follows Ohm's law [46]. The Cu leads to an improvement in weak links between grains and the compactness of the metallized Cu/PET, this ultimately enhances the electrical current. A current of $7.46\text{x}10^{-8}$ A at an applied voltage 300 V is increased to $1.52\text{x}10^{-7}$ A after 60 min of Cu deposition as shown in Table 2. The increasing behavior of electrical current with Cu deposition is attributed to increased number of charge carriers in the metallized Cu/PET. The high quality of copper coatings is the direct reason of enhanced electrical current [47].

The DC conductivity of PET also increases with Cu deposition time as shown in Fig.8. This increase in conductivity is due the creation of joint conductive state of connected CuNPs, which is a consequence of tight dispersion of CuNPs in PET matrix. Due to this homogeneous distribution of CuNPs as observed by AFM, the effective contact surface area between the CuNPs increases which subsequently reduces the resistivity. The conductivity is increased from $1.75x10^{-8}$ $S.cm^{-1}$ for pristine PET to $3.57x10^{-8}$ $S.cm^{-1}$ for 60 min Cu/PET. The formation of Cu/PET conductive network is the main cause for improvement of the DC electrical conductivity [48]. The non-linear Dc conductivity–voltage characteristics clearly show the possibility of the fabricated highly-ordered patterned CuNPs/PET finding potential applications in future nano-electronics devices.

The resistance of the PET and different deposition time of Cu/PET is shown in Fig. 9. The resistance of PET is about $4.02x10^{9}$ Ω which decreases to $1.9x10^{9}$ Ω for 60 min Cu/PET as listed in Table 2. This decrease in electrical resistance is due to the agglomeration of conductive particles in polymer matrix and carrier concentration after copper deposition [49]. Lofty et al. previously reported a decrease in the electrical resistivity of multi-walled carbon nanotube (MWCNT) embedded PVA polymer [50]. They recorded the resistance of PVA around $2.6x10^{7}$Ω decreased to $2.1x10^{5}$Ω for the MWCNT/PVA composite film. The increase in conduction pathways subsequently minimizes charge carrier scattering, thus raise the carrier mobility and reduce the electrical resistance of the prepared films. In summary, the decrease in electrical resistance is suggested to be due to the agglomeration of conductive particles in the polymer matrix in line with the literature [50].

Table 2: Electrical current, DC conductivity and electrical resistance of pristine PET and Cu/PET films at applied voltage of 300 V

	Current (A)	DC conductivity ($S.cm^{-1}$)	Resistance (Ω)
Pristine PET	7.46E-08	1.75E-8	4.02E+09
20 min Cu/PET	1.27E-07	2.98E-8	2.36E+09
40 min Cu/PET	1.49E-07	3.50E-8	2.02E+09
60 min Cu/PET	1.52E-07	3.57E-8	1.9E+09

4. Conclusion

The fabrication of reliable flexible conductive substrates is still a great challenge to overcome for widespread application and commercialization of wearable electronics. Cu deposited PET has recently received increasing interest due to its promising mechanical and electrical properties as flexible platforms

for 2D optoelectronic device applications. In this work, we demonstrated successful fabrication of Cu/PET composite substrate surfaces using an easy to operate and control home-made ion beam sputtering system. The morphological, structural, mechanical and electrical properties of PET at 20, 40 and 60 min of Cu deposition time are investigated. All the mentioned properties of PET are found to be modified by deposition of Cu to different extents with increasing deposition time. The roughness and adhesion of Cu/PET surface, each, is found to increase until a deposition time of 40 min to about twice of corresponding pristine PET values, and then to decrease again at 60 min. The Young's modulus is found to follow a similar trend with increasing deposition time which means Cu deposited surface can remain to be soft and not become brittle with increasing deposition time, which is a desired mechanical property for flexible electronic applications. The resistance is found to decrease and DC conductivity is found to increase steadily due to continuous network formation between CuNPs with increasing deposition time. Increased occurrence of PET defects with high momentum impact of Cu deposition in time is suggested to promote densification of nucleation sites for CuNPs formation which eventually result in aggregate connectivity and increased conduction pathway formation which improves overall electrical properties. I-V measurements proved that all Cu/PET samples retained their Ohmic nature throughout an applied electrical potential range of 0-300 V. Our results demonstrate that ion beam sputtering based Cu deposition on PET substrates has strong positive impacts on surface properties, both mechanical and electrical. By optimization of Cu deposition duration, both the desired mechanical properties such as increased adhesion force beside Young's modulus, and desired electrical properties such as increased DC conductivity and decreased resistance can be maintained in Cu/PET platform.

Declarations

Acknowledgments:

The authors extend their appreciation to the Deanship of Scientific Research at Jouf University for funding this work through research grant no (DSR2020-02-447).

References

[1] Li, M., Yang, K., Zhu, W., Shen, J., Rollinson, J., Hella, M., & Lian, J. (2020). Copper-Coated Reduced Graphene Oxide Fiber Mesh-Polymer Composite Films for Electromagnetic Interference Shielding. *ACS Applied Nano Materials*, *3*(6), 5565-5574.

[2] Li, Y., Wu, M., Sun, Y., & Yu, S. (2019). High-performance flexible transparent conductive thin films on PET substrates with a CuM/AZO structure. Journal of Materials Science: Materials in Electronics, 30(14), 13271-13279.

[3] Klein, E., Huber, K., Paul, O., & Ruther, P. (2020). Low-temperature plasma annealing of sputtered indium tin oxide for transparent and conductive thin-films on glass and polymer substrates. Thin Solid Films, 693, 137715.

[4] Sportelli, M. C., Valentini, M., Picca, R. A., Milella, A., Nacci, A., Valentini, A., & Cioffi, N. (2018). New insights in the ion beam sputtering deposition of ZnO-fluoropolymer nanocomposites. Applied Sciences, 8(1), 77.

[5] Zhu, J., Hu, Y., Xu, M., Yang, W., Fu, L., Li, D., & Zhou, L. (2018). Enhancement of the adhesive strength between Ag films and Mo substrate by Ag implanted via ion beam-assisted deposition. Materials, 11(5), 762.

[6] Faÿ, F., Poncin-Epaillard, F., Le Norcy, T., Linossier, I., & Réhel, K. (2020). Surface Plasma Treatment (Ar/CF4) Decreases Biofouling on Polycarbonate Surfaces. Surface Innovations, 1-12.

[7] Atta, Ali, Salah Lotfy, and Eslam Abdeltwab. "Dielectric properties of irradiated polymer/multiwalled carbon nanotube and its amino functionalized form." Journal of Applied Polymer Science 135.33 (2018): 46647y

[8] Samipour, S., Taghvaei, H., Mohebbi-Kalhori, D., & Rahimpour, M. R. (2019). Plasma treatment and chitosan coating: a combination for improving PET surface properties. Surface Innovations, 8(1–2), 76-88

[9] Bertrand, Patrick, P. Lambert, and Y. Travaly. "Polymer metallization: Low energy ion beam surface modification to improve adhesion." Nuclear Instruments and Methods in Physics Research Section B: Beam Interactions with Materials and Atoms 131.1-4 (1997): 71-78.

[10] Li, Dongdong, et al. "Printable transparent conductive films for flexible electronics." Advanced Materials 30.10 (2018): 1704738.

[11] Akl, Alaa A., et al. "Improving microstructural properties and minimizing crystal imperfections of nanocrystalline Cu2O thin films of different solution molarities for solar cell applications." Materials Science in Semiconductor Processing 74 (2018): 183-192.

[12] Kumari, S., et al. "Enhanced corrosion resistance and mechanical properties of nanostructured graphene-polymer composite coating on copper by electrophoretic deposition." Journal of Coatings Technology and Research 15.3 (2018): 583-592

[13] Wang, Hu, et al. "Improvement of interfacial interaction and mechanical properties in copper matrix composites reinforced with copper coated carbon nanotubes." Materials Science and Engineering: A 715 (2018): 163-173.

[14] Madhusudanan, Sreejith P., Kallol Mohanta, and Sudip K. Batabyal. "Electrical bistability and memory switching phenomenon in Cu 2 FeSnS 4 thin films: role of pn junction." Journal of Solid State Electrochemistry 23.5 (2019): 1307-1314

[15] Kannan, R., et al. "Effect of tungsten (W) on structural and magnetic properties of electroplated NiFe thin films for MEMS applications." Materials Research Express 5.4 (2018): 046414..

[16 Kim, Ki-Joong, et al. "Metal–organic framework thin film coated optical fiber sensors: a novel waveguide-based chemical sensing platform." ACS sensors 3.2 (2018): 386-394

[17] Huang, Jinhua, et al. "Seed-layer-free growth of ultra-thin Ag transparent conductive films imparts flexibility to polymer solar cells." Solar Energy Materials and Solar Cells 184 (2018): 73-81

[18] Raut, N. C., and K. Al-Shamery. "Inkjet printing metals on flexible materials for plastic and paper electronics." Journal of Materials Chemistry C 6.7 (2018): 1618-1641

[19] Huang, X., Zhang, F., Liu, Y., & Leng, J. (2020). Active and deformable organic electronic devices based on conductive shape memory polyimide. *ACS applied materials & interfaces*, *12*(20), 23236-23243.

[20] Back, Seunghyun, and Bongchul Kang. "Low-cost optical fabrication of flexible copper electrode via laser-induced reductive sintering and adhesive transfer." Optics and Lasers in Engineering 101 (2018): 78-84

[21] Atta, A. (2020). Enhanced dielectric properties of flexible Cu/polymer nanocomposite films. Surface Innovations, 9(1), 17-24

[22] Koo, Seok-Bon, et al. "Study on Aging Effect of Adhesion Strength Between Polyimide Film and Copper Layer." Metals and Materials International 25.1 (2019): 117-126.

[23] Xu, WenZheng, et al. "Characterisation of PET nonwoven deposited with Ag/FC nanocomposite films." Surface Engineering 34.11 (2018): 838-845

[24] Kobayashi, T., et al. "DEFECTS IN ALUMINUM THIN FILMS DEPOSITED ON PET SUBSTRATE AND THEIR FORMATION MECHANISM." Journal of Advanced Manufacturing Technology (JAMT) 13.1 (2019): 71-82.

[25] Zhang, Yang, and Zhixin Kang. "Highly conductive and anticorrosion Ag/CNTs/NDs hybrid films on molecular-grafted PET substrate for flexible electrodes." Applied Surface Science 427 (2018): 282-292.

[26] Kim, Young Seok, et al. "Investigation of structure and mechanical properties of TiZrHfNiCuCo high entropy alloy thin films synthesized by magnetron sputtering." Journal of Alloys and Compounds 797 (2019): 834-8.

[27] Mwema, Fredrick Madaraka, et al. "Properties of physically deposited thin aluminium film coatings: A review." Journal of alloys and compounds 747 (2018): 306-323.

[28] Rousta, Abrisham, Davoud Dorranian, and Mohammad Elahi. "Electrophoretic deposition of cobalt oxide nanoparticles on aluminium substrate." Surface Engineering (2019): 1-10.

[29] Abdel Reheem, A. M., A. Atta, and Mahmmoud S. Abd-Elmonem. "Irradiation and silver deposition for improvement of nasopharyngeal airway medical device properties." Surface Review and Letters 24.03

(2017): 1750031..

[30] Liu, Xuqing, et al. "Durable, Washable, and Flexible Conductive PET Fabrics Designed by Fiber Interfacial Molecular Engineering." Macromolecular Materials and Engineering 301.11 (2016): 1383-1389

[31] Abdel-Fattah, E., A. I. Alharthi, and T. Fahmy. "Spectroscopic, optical and thermal characterization of polyvinyl chloride-based plasma-functionalized MWCNTs composite thin films." Applied Physics A 125.7 (2019): 475

[32] Oh, Hyo-Jun, et al. "Effect of various seed metals on uniformity of Ag layer formed by atmospheric plasma reduction on polyethylene terephthalate substrate: An application to electromagnetic interference shielding effectiveness." Thin Solid Films 676 (2019): 75-86.

[33] Atta A, ABDEL REHEEM AM, and Abdeltwab E. Ion Beam Irradiation Effects on Surface Morphology and Optical Properties of ZnO/PVA Composites. Surface Review and Letters (2020): 1950214.

[34] Shi, Yu-E., et al. "Copper-Nanocluster-Based Transparent Ultraviolet-Shielding Polymer Films." ChemNanoMat 5.1 (2019): 110-11.

[35] Abdel-Galil, A., A. Atta, and M. R. Balboul. "Effect of low energy oxygen ion beam treatment on the structural and physical properties of ZnO thin films." *Surface Review and Letters* (2020).

[36] Xiong, Pengpeng, et al. "Transparent electrodes based on ultrathin/ultra smooth Cu films produced through atomic layer deposition as new ITO-free organic light-emitting devices." Organic Electronics 58 (2018): 18-24.

[37] Atta, Ali, et al. "Modulation of structure, morphology and wettability of polytetrafluoroethylene surface by low energy ion beam irradiation." Nuclear Instruments and Methods in Physics Research Section B: Beam Interactions with Materials and Atoms 300 (2013): 46-53.

[38 Nasar, Gulfam, et al. "Structural and electromechanical behavior evaluation of polymer-copper nanocomposites." Macromolecular Research 24.4 (2016): 309-313. [39] Reheem, AM Abdel, MIA Abdel Maksoud, and A. H. Ashour. "Surface modification and metallization of polycarbonate using low energy ion beam." Radiation Physics and Chemistry 125 (2016): 171-175

[40] Park, Won-Hwa. "Electrical performance of chemical vapor deposition graphene on PET substrate tailored by Cu foils surface morphology." The European Physical Journal-Applied Physics 67.3 (2014)

[41] Abdel-Galil A, Atta A and Balboul MR. Effect of low energy oxygen ion beam treatment on the structural and physical properties of ZnO thin films. Surface Review and Letters (2020).

[42] Cho, Kyung-Su, et al. "Highly flexible and semi-transparent Ag–Cu alloy electrodes for high performance flexible thin film heaters." RSC advances 7.72 (2017): 45484-45494.

[43] Chen, Huiyu, Yu Tai, and Chunju Xu. "Fabrication of copper-coated glass fabric composites through electroless plating process." Journal of Materials Science: Materials in Electronics 28.1 (2017): 798-802.

[44] Bistričić, Lahorija, et al. "Raman spectra, thermal and mechanical properties of poly (ethylene terephthalate) carbon-based nanocomposite films." Journal of polymer research 22.3 (2015): 39.

[45] Ding, Su, et al. "Highly conductive and transparent copper nanowire electrodes on surface coated flexible and heat-sensitive substrates." RSC advances 8.4 (2018): 2109-2115.

[46] Salem, Kh Samaher, et al. "The effect of multiwall carbon nanotube additions on the thermo-mechanical, electrical, and morphological properties of gelatin–polyvinyl alcohol blend nanocomposite." Journal of Composite Materials 49.11 (2015): 1379-1391.

[47] Li, X. F., et al. "Nickel and silver coated nano-SiO2 with excellent conductivity and permeability." Surface Engineering 31.6 (2015): 427-432.

[48] Xue, Qingzhong, and Jin Sun. "Electrical conductivity and percolation behavior of polymer nanocomposites." Polymer nanocomposites. Springer, Cham, 2016. 51-82.

[49] Kim, Sang Hoon, et al. "Improved electrical and thermo-mechanical properties of a MWCNT/In–Sn–Bi composite solder reflowing on a flexible PET substrate." Scientific reports 7.1 (2017): 1-14.

[50] Lotfy, S., A. Atta, and E. Abdeltwab. "Comparative study of gamma and ion beam irradiation of polymeric nanocomposite on electrical conductivity." Journal of Applied Polymer Science 135.15 (2018): 46146

Figures

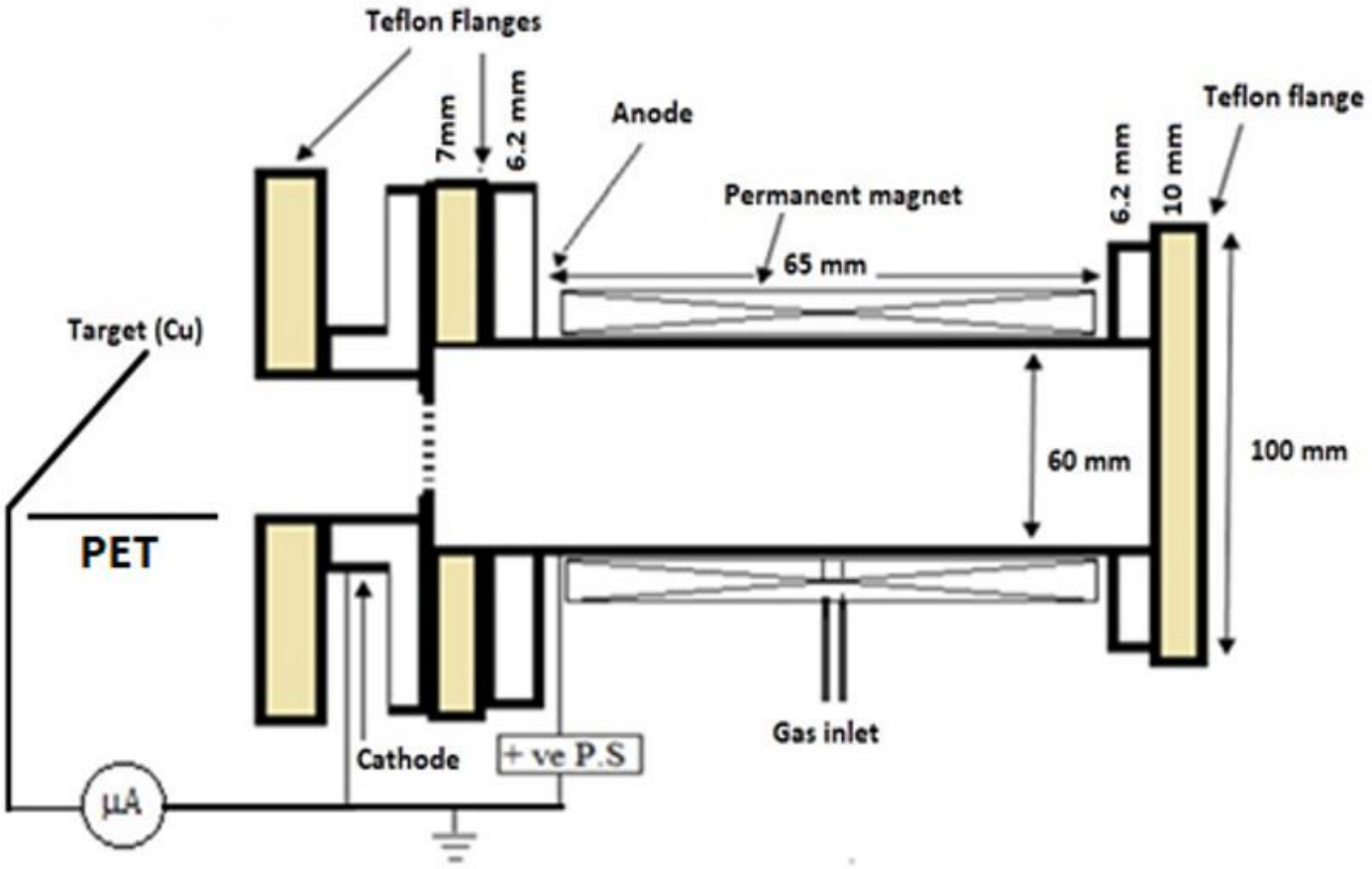

Figure 1

Cold cathode broad beam ion source with Cu sputtering target.

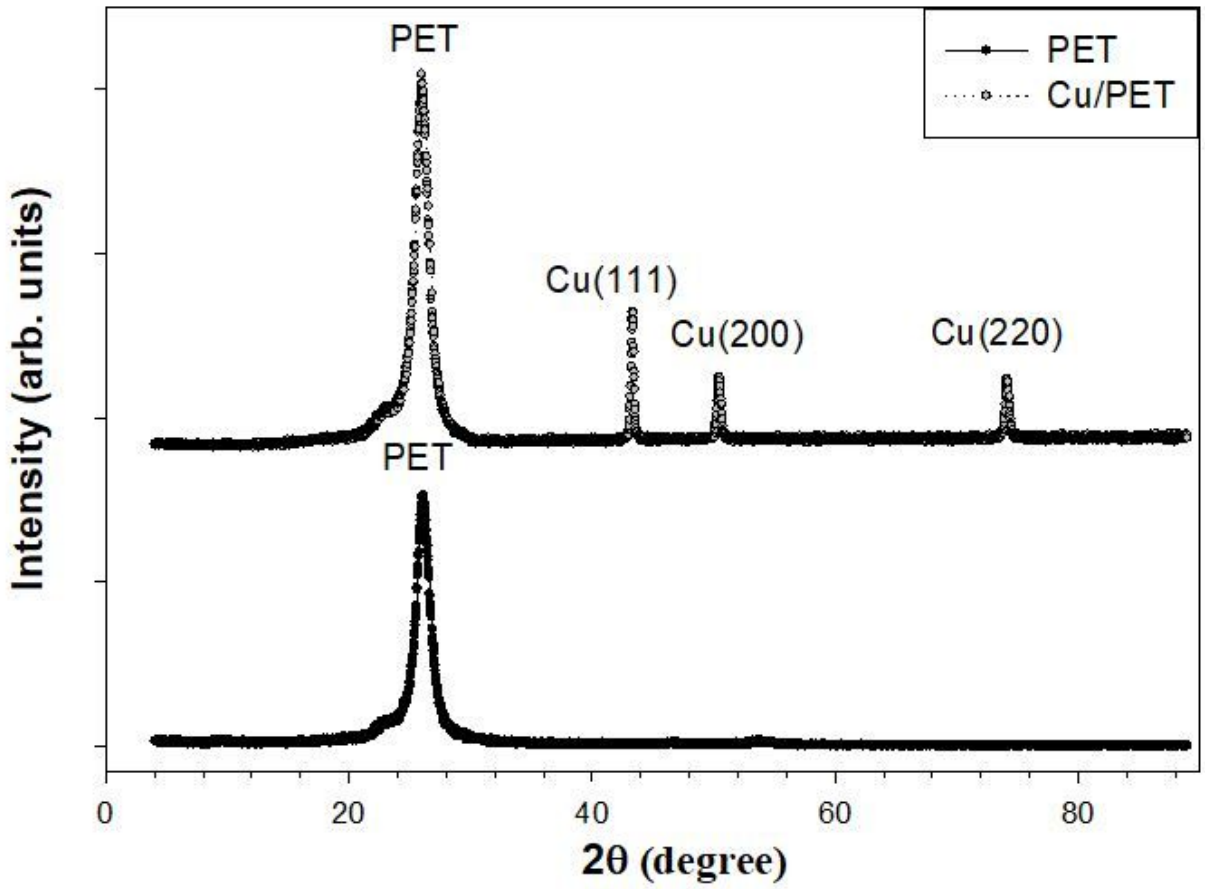

Figure 2

The XRD pattern of pristine PET and Cu/PET films.

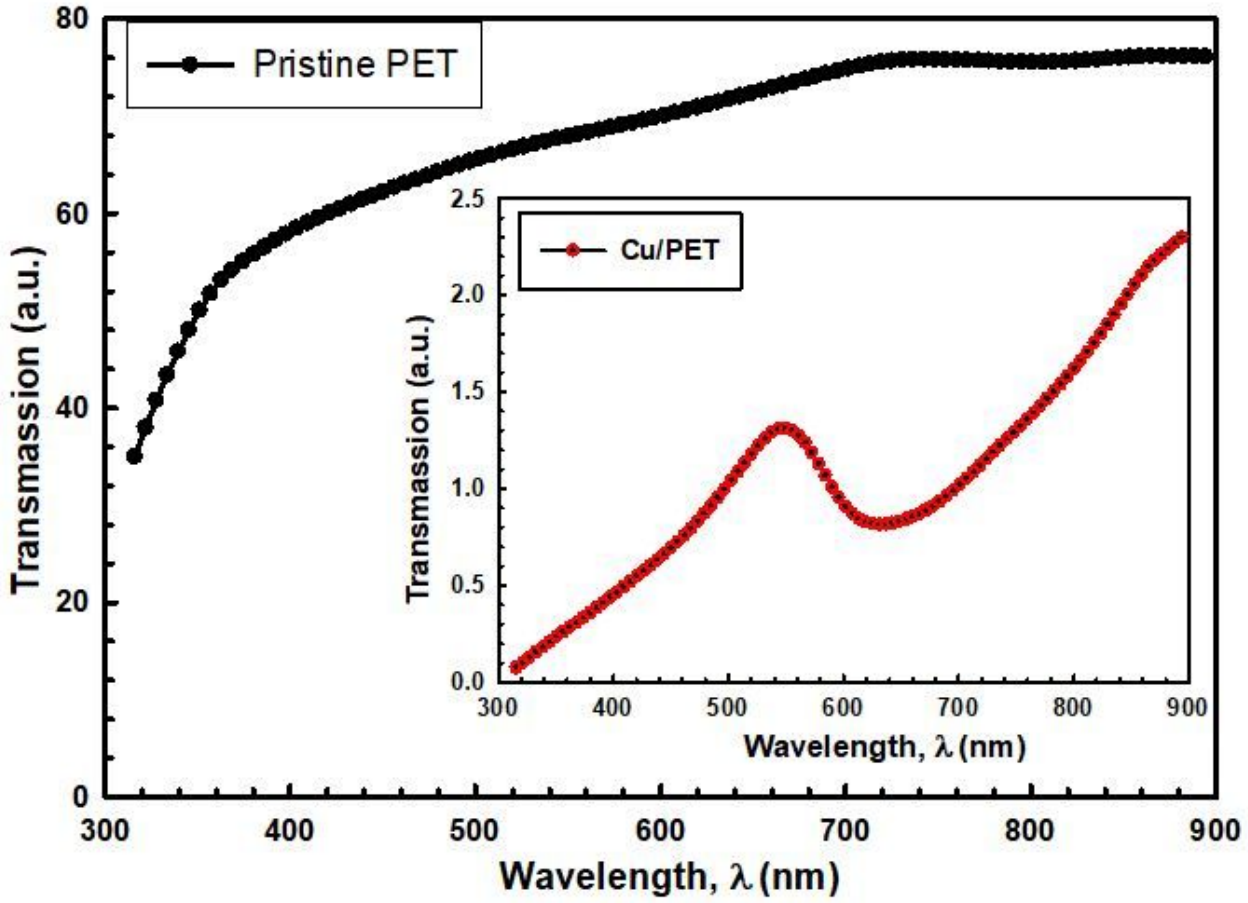

Figure 3

UV/Vis transmittance spectra of pristine PET and Cu/PET films.

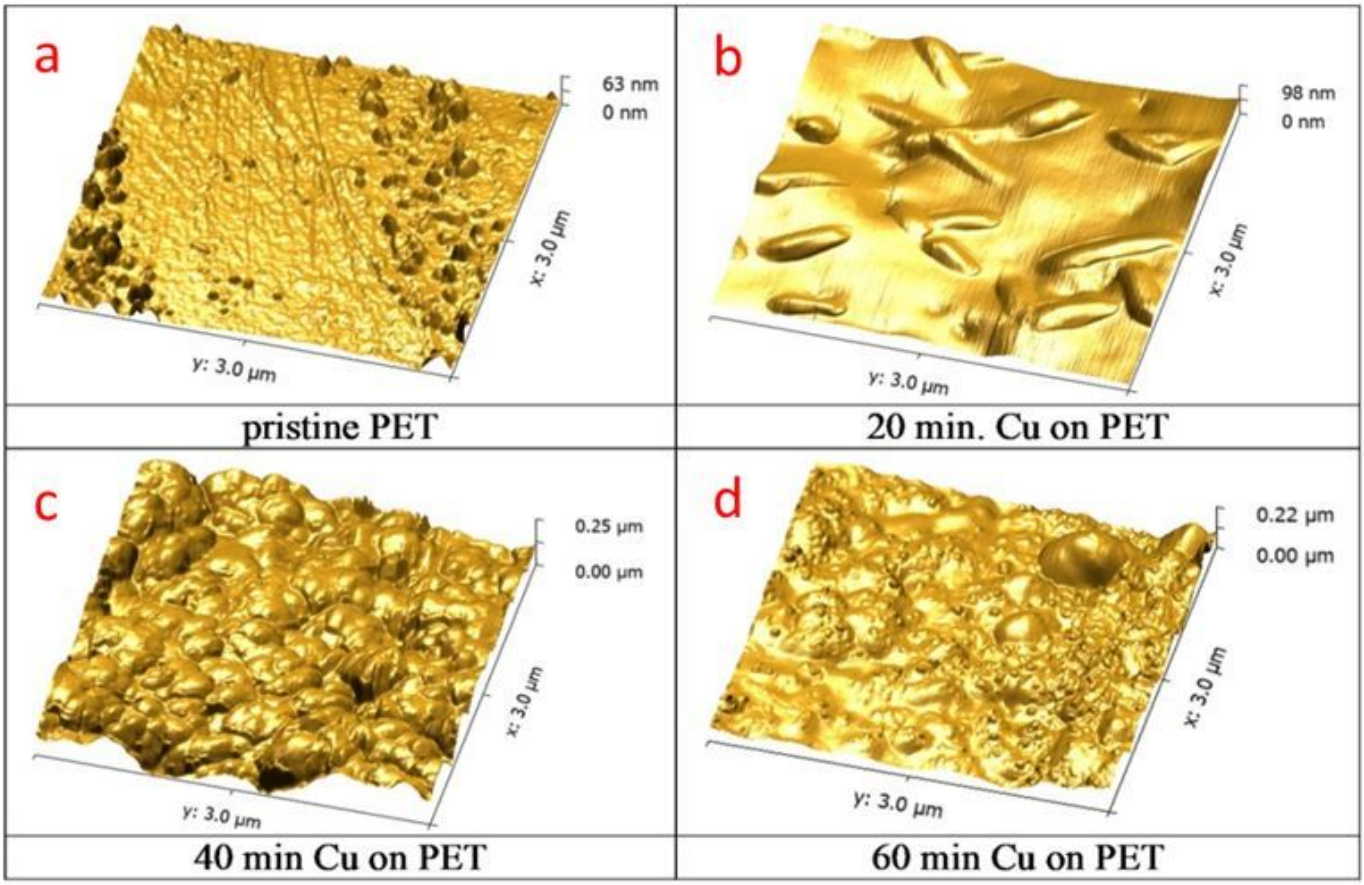

Figure 4

AFM images of (a) pristine PET, (b) 20 min Cu/PET, (c) 40 min Cu/PET and (d) 60 min Cu/PET.

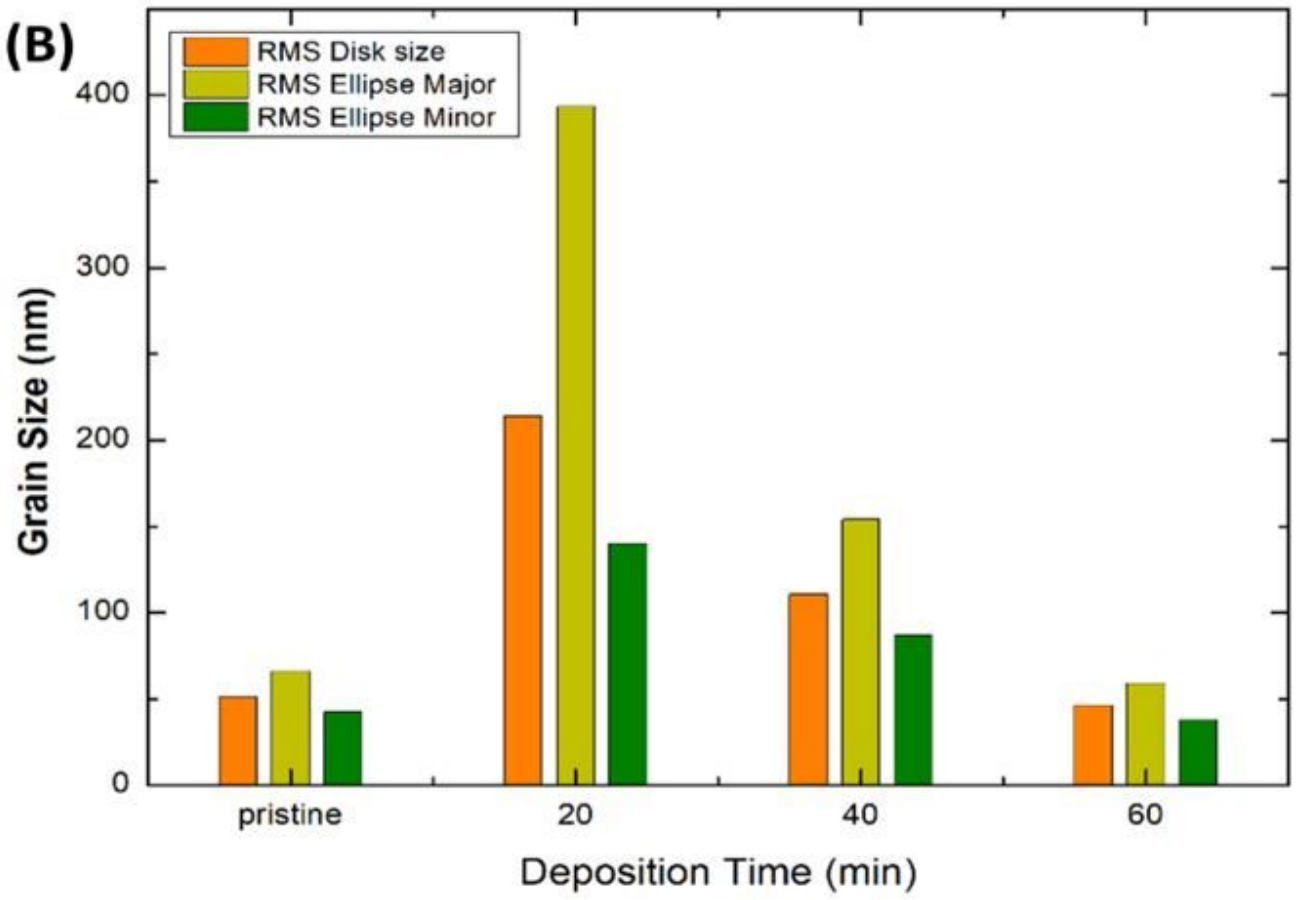

Figure 5

The grain analysis of pristine PET and Cu/PET films.

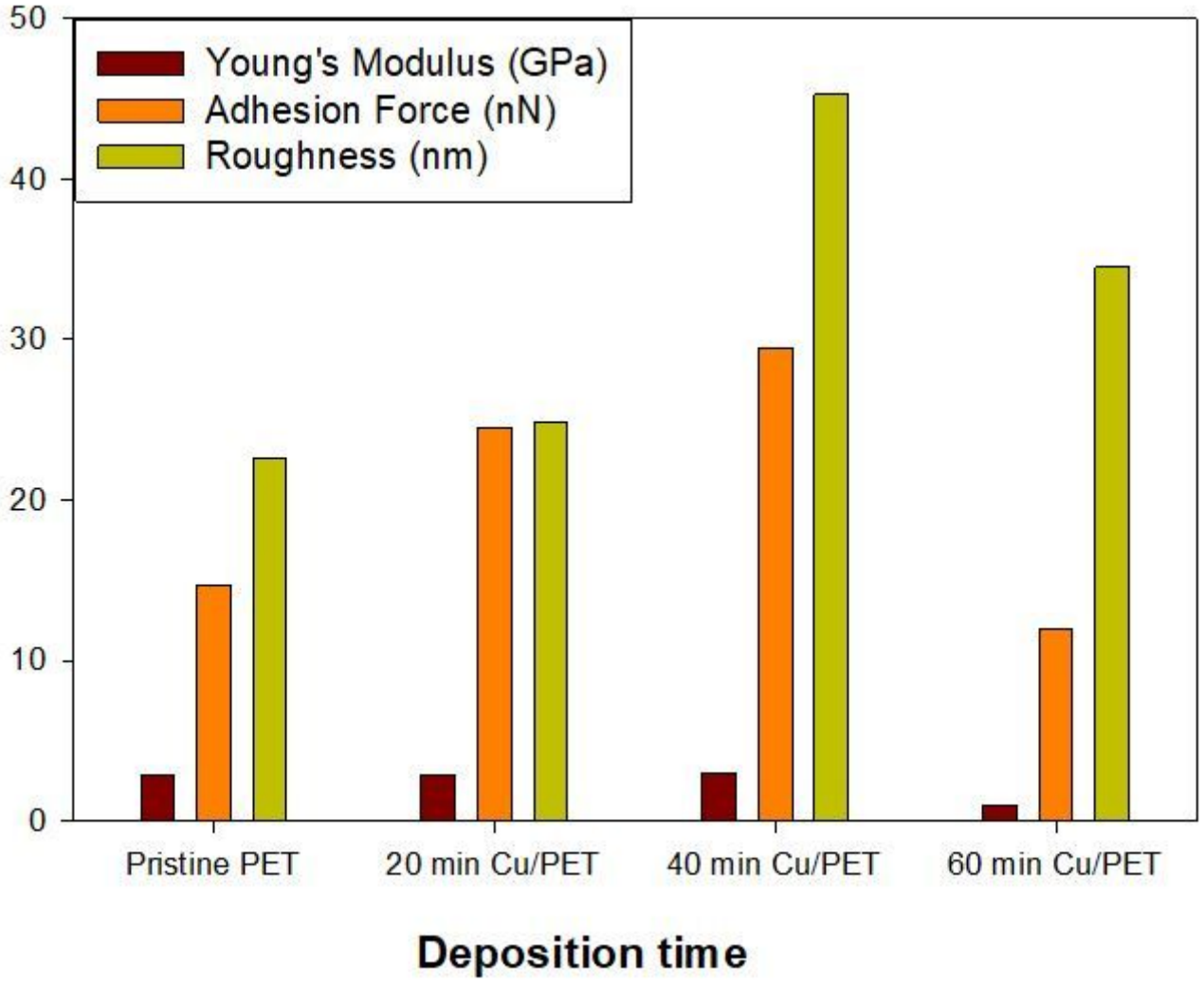

Figure 6

The Young's modulus (GPa), adhesion force (nN) and surface roughness (nm) for pristine PET and Cu/PET films.

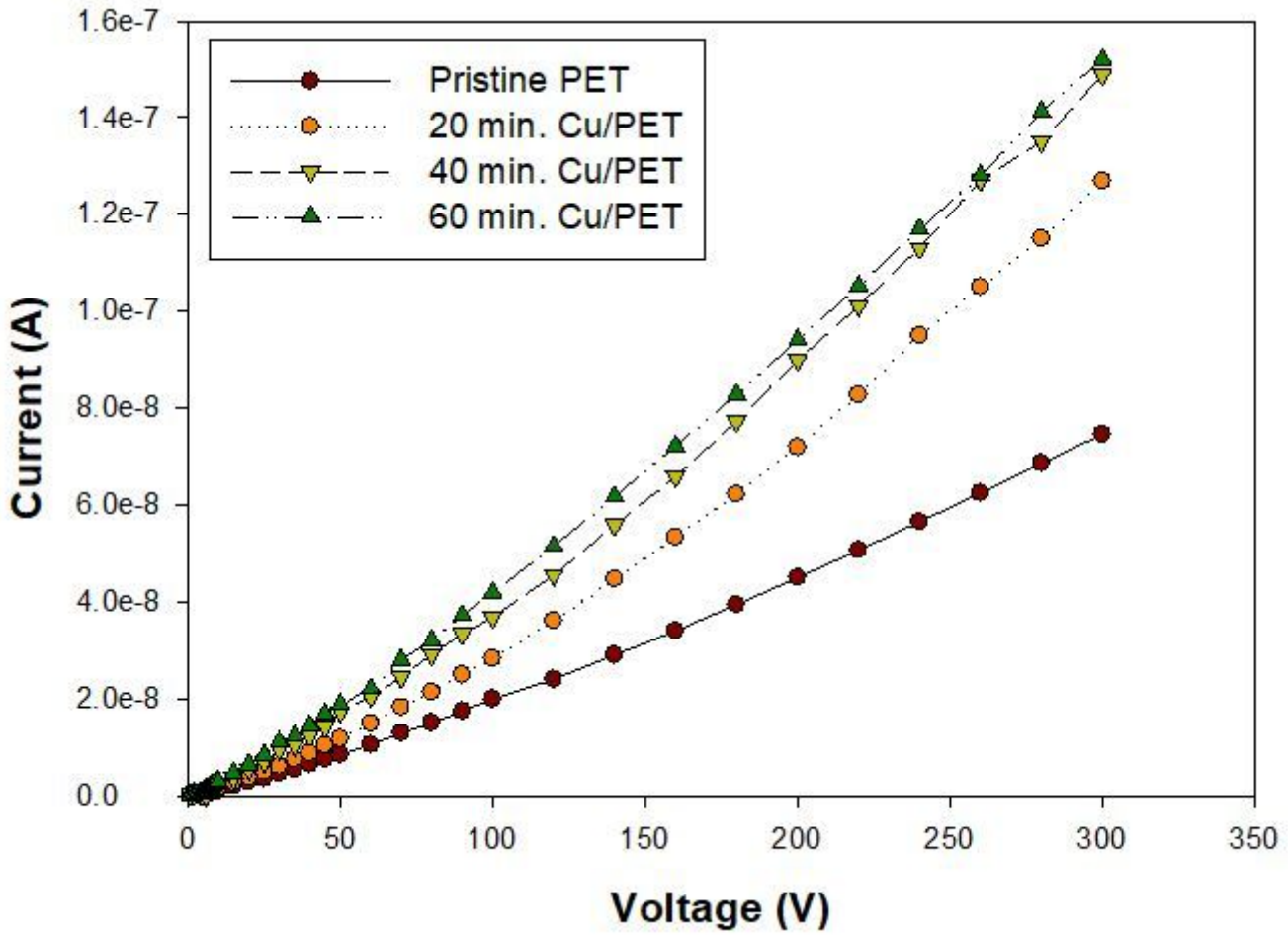

Figure 7

Current–voltage characteristic curve of pristine PET and Cu/PET films.

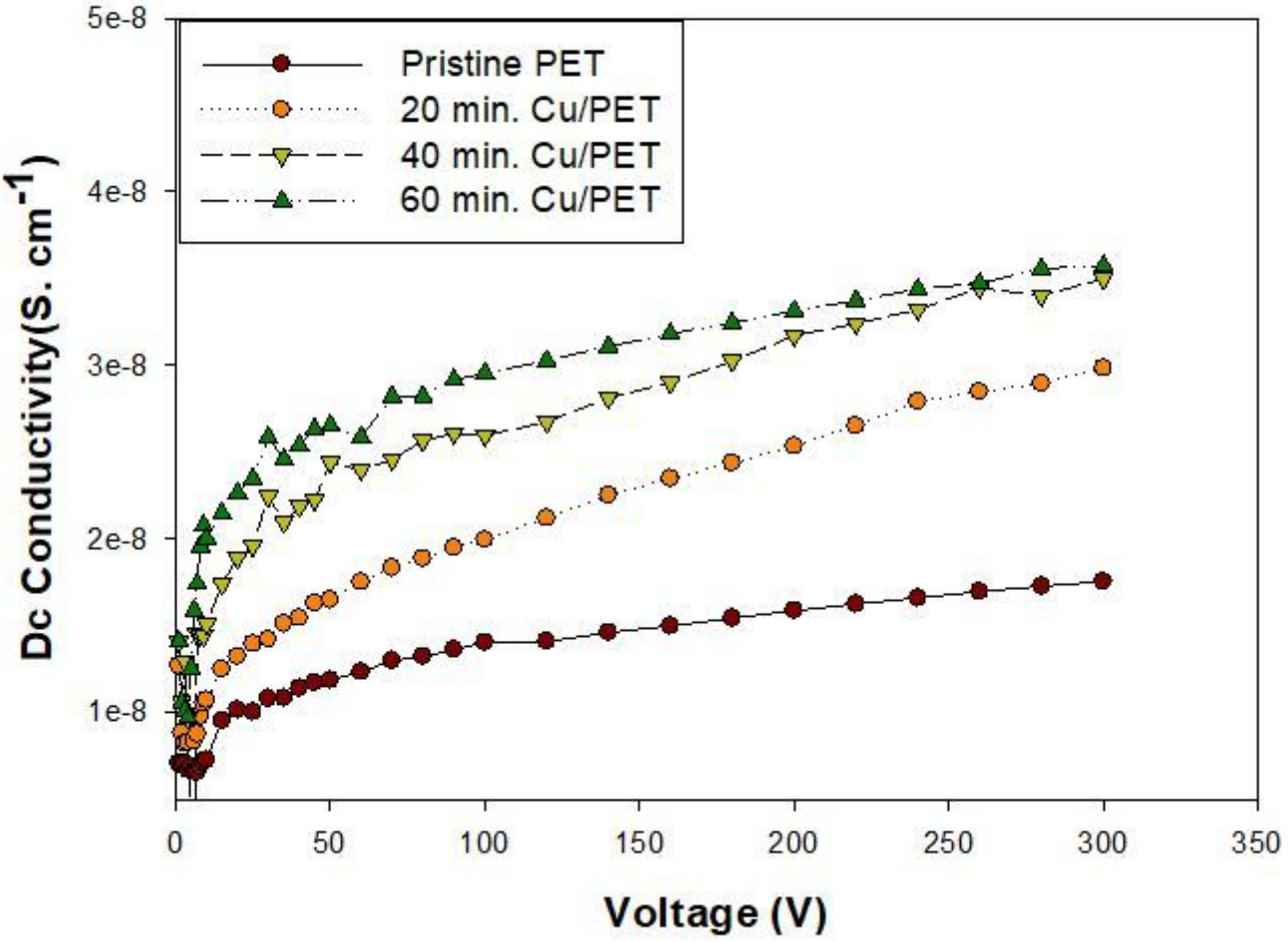

Figure 8

Dc conductivity versus applied voltage of pristine PET and Cu/PET films.

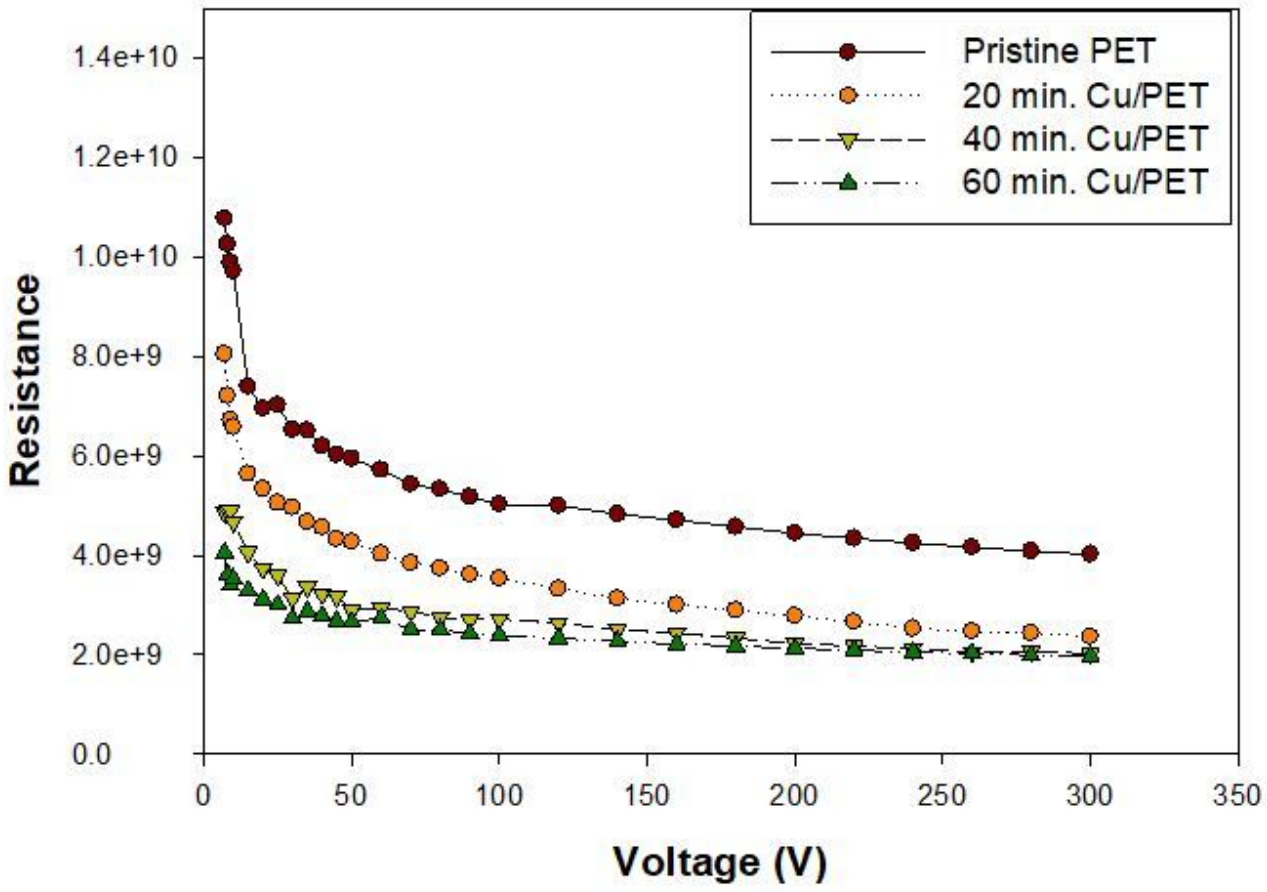

Figure 9

Resistance–voltage characteristics of pristine PET and Cu/PET films.